Applied Organometallic Chemistry

WILEY

Applied Organometallic Chemistry

RESEARCH ARTICLE OPEN ACCESS

Dendritic, Water-Soluble, and Nonaggregated Axially Substituted Silicon Phthalocyanine as Potential Endometrial Anticancer Agent

Turgut Keles[1] | Gökçe Seyhan[2] | Zekeriya Biyiklioglu[3] | Kübra Kolci[4,5] | Rengin Reis[4] | Burak Barut[2]

[1]Central Research Laboratory Application and Research Center, Recep Tayyip Erdoğan University, Rize, Türkiye | [2]Faculty of Pharmacy, Department of Biochemistry, Karadeniz Technical University, Trabzon, Türkiye | [3]Faculty of Science, Department of Chemistry, Karadeniz Technical University, Trabzon, Türkiye | [4]Faculty of Pharmacy, Department of Toxicology, Acibadem Mehmet Ali Aydinlar University, Istanbul, Türkiye | [5]Faculty of Pharmacy, Department of Toxicology, Yeditepe University, Istanbul, Türkiye

Correspondence: Zekeriya Biyiklioglu (zekeriyab@ktu.edu.tr)

Received: 12 June 2024 | **Revised:** 23 July 2024 | **Accepted:** 3 August 2024

Funding: The authors received no specific funding for this work.

Keywords: endometrial cancer | photodynamic therapy | phthalocyanine | silicon | synthesis

ABSTRACT

In this work, dendritic, water-soluble, and nonaggregated axially substituted silicon phthalocyanines (**EA-TD-Si** and **EA-TD-SiQ**) were synthesized and characterized. Then, the supercoiled pBR322 plasmid DNA damage properties of **EA-TD-Si** and **EA-TD-SiQ** were examined using agarose gel electrophoresis without light irradiation. In addition, the cytotoxicity and phototoxicity of **EA-TD-Si** and **EA-TD-SiQ** on human endometrium adenocarcinoma (HEC-1B) cells were investigated using an MTT assay. The results indicated that **EA-TD-SiQ** had high photodamage properties via singlet oxygen depending on the light dose, while **EA-TD-Si** did not show any DNA damage without light. In addition, **EA-TD-SiQ** had higher phototoxic effects than **EA-TD-Si** on HEC-1B cells according to the MTT assay. These results revealed the potential of **EA-TD-SiQ** to be used as a PDT agent in endometrial cancer.

1 | Introduction

Endometrial cancer (EC) is one of the most common gynecologic malignancies that can be seen in women around the world. It has been reported that more than 400,000 women were diagnosed with EC in 2020 and 100,000 women died due to this disease [1, 2]. It is known that the incidence and mortality of the disease are increasing day by day. Genetic predisposition, age, obesity, and insulin resistance-like factors make EC a multietiological disease. It can be divided into two types according to the prognosis and histopathology [3]. While Type 1 is caused by unopposed estrogen and is diagnosed at a young age, early-stage or low-grade patients can be treated surgically. Type 2 occurs with atrophic endometrium, and it has a poor prognosis since it can be diagnosed at an advanced stage in the elderly [4]. In general, ~80% of cases are diagnosed early, while 3%–14% are diagnosed before the age of 40 [5]. Once diagnosed, the first step of the EC treatment is surgery, but in cases of disease progression and relapse, other treatment methods such as chemotherapy and radiotherapy can also be used. In addition, the use of immunotherapy and targeted therapies, which are two novel methods, have become more effective and interesting methods after the first step of treatments in recent years [6]. Compared

Abbreviations: °C, degree Celsius; BEAS-2B, human bronchial epithelial cells; D_2O, deuterium oxide; DMF, dimethylformamide; DMSO-d6, dimethyl sulfoxide-d6; DNA, deoxyribonucleic acid; EA-D-Cl, 3,3′-[[5-(chloromethyl)-1,3-phenylene]bis (oxypropane-3,1-diyloxy)]bis(N,N-diethylaniline); EA-TD-OH, {3,5-bis[(3,5-bis{3-[3 (diethylamino)phenoxy]propoxy}benzyl)oxy] phenyl}methanol; EA-TD-Si, Silicon (IV) phthalocyanine; EA-TD-SiQ, Water soluble silicon (IV) phthalocyanine; EC, endometrial cancer; FDA, Food and Drug Administration; g, gram; HEC-1B, human endometrium adenocarcinoma cells; HeLa, human cervical carcinoma cells; IR, infrared; KOH, potassium hydroxide; MB, methylene blue; min, minutes; mL, milliliter; mp, melting point; MTT, 3-(4,5-dimethylthiazol-2-yl)-2,5-diphenyltetrazolium bromide; *m/z*, mass-to-charge ratio; NaH, sodium hydride; NaN_3, sodium azide; NMR, nuclear magnetic resonance; PDT, photodynamic therapy; ppm, parts per million; PSs, photosensitizers; $SiPcCl_2$, silicon phthalocyanine dichloride; $SOCl_2$, thionyl chloride.

to classical methods, photodynamic therapy (PDT) has gained more attention from researchers due to its minimal invasiveness, high tumor selectivity, low systemic toxicity, and ability to induce cell death without causing drug resistance [7, 8].

PDT is a Food and Drug Administration (FDA)-approved therapy that is being investigated in preclinical and clinical settings for managing various diseases and cancer types [9]. Among these types, it has been reported to be effective for gynecological malignancies such as cervical and vulvar cancers, as well as early-stage EC [5]. In this method, reactive oxygen species are formed as a result of the reaction of a nontoxic photosensitizer (PS) excited by a specific wavelength of light with molecular oxygen. These molecules are cytotoxic and induce cell death by causing oxidative damage in cancer cells [10]. Cell death resulting from PDT can take the form of apoptosis, necrosis, or autophagy. The type of cell death is determined by the dose of the PS and the light used [11].

PSs are crucial in the application of PDT for EC treatment. Raab et al. found that hematoporphyrin derivatives had a lethal effect on EC cells (HEC1-1A) [12]. In a study by Schneider-Yin et al. using the same cells, 5-aminolevulinic acid and hypericin were applied alone and in combination [13]. It was observed that their combinations showed higher phototoxic effects. In another study, Ziółkowski et al. treated Grade 1 cancerous tissues with hematoporphyrin derivatives [14]. The results showed an increase in necrosis and a decrease in proliferation and epidermal growth factor. In another study, Choi et al. demonstrated that the application of PDT to young patients with early-stage EC may be an effective preventive treatment method to preserve fertility [15]. In a different study, Godoy et al. applied Photofrin II, a hematoporphyrin derivative, to a group including EC patients and then exposed the tumor tissue to 630 nm of visible light [16]. There are several side effects, such as burning sensation, pain, and edema, that have been observed in the PDT treatment. For this reason, the search for alternative drug molecules with a low side effect profile continues.

Ideally, PSs should possess features such as ease of obtainment, pure chemical form, solubility and stability in physiological environments, minimal toxicity in the dark, and rapid excretion from the body after treatment [17]. Phthalocyanines are second-generation PSs with an 18-π electron system that exhibit strong absorption in the visible region of the electromagnetic spectrum [18]. Phthalocyanines are considered good candidates due to their high absorption at 600–850 nm, which is referred to as the "phototherapeutic window," and their high capacity for singlet oxygen production [19]. Nevertheless, their hydrophobic structure, low solubility, and tendency to aggregate limit their use. This situation is attempted to be overcome by adding substituents to their structure or by changing the central metal ion [20]. In this paper, we investigated the potential of **EA-TD-Si** and **EA-TD-SiQ** for PDT in the EC treatment.

2 | Materials and Methods

The materials, equipment, DNA damage properties, and cytotoxicity/phototoxicity determined by the 3-(4,5-dimethylthiazol-2-yl)-2,5-diphenyltetrazolium bromide (MTT) assay of the compounds were presented as supporting information.

2.1 | Synthesis

2.1.1 | Synthesis of 3,3′-[[5-(Chloromethyl)-1,3-Phenylene]Bis (Oxypropane-3,1-Diyloxy)] Bis(N,N-Diethylaniline) (EA-D-Cl)

EA-D-OH (1 g, 1.82 mmol) was dissolved in 10 mL of chloroform in a 100 mL glass flask. 0.3 mL (3 mmol) of $SOCl_2$ was added with the aid of a dropping funnel at room temperature and refluxed at 65°C for 1 day. The reaction mixture was cooled to 0°C, and a 50% KOH solution was added to make it basic. The mixture was extracted with chloroform and water. For the purification process, the column was made of aluminum oxide by using chloroform as a solvent. Yield: 700 mg (68%). IR (ATR), ν/cm^{-1}: 3087 (Ar–H), 2963–2850 (Aliph. C–H), 1594, 1499, 1461, 1375, 1354, 1287, 1259, 1214, 1165, 1063, 1015, 790, 752, 713, 686. ^{1}H NMR (400 MHz, DMSO-d_6), (δ): 6.99 (t, 2H, Ar–H), 6.59 (d, 2H, Ar–H), 6.47 (s, 2H, Ar–H), 6.22 (m, 2H, Ar–H), 6.14 (m, 3H, Ar–H), 4.57 (s, 2H, CH_2–Cl), 4.10–4.05 (m, 8H, CH_2–O), 3.27–3.22 (q, 4H, CH_2–N), 2.11–2.08 (m, 4H, CH_2), 1.02 (t, 12H, CH_3). ^{13}C NMR (100 MHz, DMSO-d_6), (δ): 160.20, 160.10, 154.84, 149.14, 130.25, 107.68, 105.17, 105.15, 101.17, 98.61, 67.78, 64.87, 64.11, 44.28, 29.15, 12.87. MS (ESI), (m/z) calcl. 568.31; found: 569.36 $[M+H]^+$.

2.1.2 | {3,5-Bis[(3,5-Bis{3-[3 (Diethylamino)Phenoxy] Propoxy}Benzyl)Oxy]Phenyl}Methanol (EA-TD-OH)

3,5-Dihydroxy benzyl alcohol (89 mg, 0.6 mmol) and dry potassium carbonate (900 mg, 6.4 mmol) were dissolved in 90 mL of acetone. Then, **EA-D-Cl** (700 mg, 1.23 mmol) and 18-crown-6 (186 mg, 0.71 mmol) were added to the reaction mixture. The reaction mixture was refluxed for 2 days at 70°C under a nitrogen atmosphere. The crude **EA-TD-OH** was purified with column chromatography on silica gel by using chloroform as a solvent. Yield: 400 mg (54%). IR (ATR), ν/cm^{-1}: 3456 (OH), 3085 (Ar–H), 2968–2875 (Aliph. C–H), 1702, 1593, 1499, 1450, 1374, 1356, 1287, 1213, 1161, 1062, 952, 829, 747, 686, 616. ^{1}H NMR (400 MHz, DMSO-d_6), (δ): 6.98 (t, 4H, Ar–H), 6.58 (d, 4H, Ar–H), 6.54 (s, 3H, Ar–H), 6.45 (s, 4H, Ar–H), 6.22 (m, 4H, Ar–H), 6.14 (m, 6H, Ar–H), 5.14 (s, 1H, –OH), 4.94 (s, 6H, CH_2–O), 4.09–4.02 (m, 16H, CH_2–O), 3.26–3.21 (q, 16H, CH_2–N), 2.10–2.07 (m, 8H, CH_2), 1.02 (t, 24H, CH_3). ^{13}C NMR (100 MHz, DMSO-d_6), (δ): 160.18, 160.15, 159.68, 149.14, 145.51, 139.96, 130.24, 106.28, 105.59, 105.36, 105.16, 101.19, 100.65, 98.58, 69.37, 64.76, 64.12, 44.07, 29.14, 12.81. MALDI-TOF-MS (m/z) calcl. 1205.56; found: 1205.33 $[M]^+$.

2.1.3 | Silicon (IV) Phthalocyanine (EA-TD-Si)

EA-TD-OH (100 mg, 0.083 mmol) was dissolved in 10 mL dry toluene, silicon phthalocyanine dichloride (24 mg, 0.040 mmol), and a small amount of NaH was added. The reaction mixture was refluxed at 110°C under a nitrogen atmosphere for one night. The crude **EA-TD-Si** was purified with column chromatography on silica gel by using chloroform/methanol (250:5) as a solvent system. Yield: 75 mg (61%). mp > 300°C. IR (ATR), ν/cm^{-1}: 3078 (Ar–H), 2965–2871 (Aliph. C–H), 1733, 1593, 1498, 1449, 1428, 1373, 1354, 1289, 1262, 1212, 1122, 1060, 910, 808, 736, 685. 646. ^{1}H NMR (400 MHz, $CDCl_3$), (δ): 9.57 (bs, 8H, Pc-H_α), 8.24 (bs, 8H, H_β), 7.10 (t, 10H, Ar–H), 6.30–6.24 (m, 40H,

Ar–H), 4.14–4.11 (m, 32H, CH_2-O), 3.99 (s, 8H, Ar-CH_2-O), 3.30–3.29 (q, 32H, CH_2–N), 2.24 (m, 16H, –CH_2–), 1.12 (t, 48H, CH_3), −0.68 (s, 4H, Si–O–CH_2). ^{13}C NMR (100 MHz, $CDCl_3$), (δ): 160.21, 160.18, 160.00, 158.23, 149.43, 149.19, 139.18, 135.97, 134.28, 130.91, 129.88, 123.57, 105.80, 105.42, 105.15, 100.75, 100.52, 98.89, 68.88, 64.65, 64.22, 44.36, 29.44, 12.63. UV–Vis (DMF) λmax (logε): 679 (4.99), 611 (4.28), 353 (4.56). MALDI-TOF-MS (*m/z*) calcl. 2949.72; found: 2949.03 $[M]^+$.

2.1.4 | Water Soluble Silicon (IV) Phthalocyanine (EA-TD-SiQ)

EA-TD-Si (23 mg, 0.007 mmol), 3 mL of chloroform, and 2.5 mL of iodomethane were mixed in a 50 mL flask at room temperature in the dark for 6 days. The reaction mixture was filtered through a glass crucible, washed with chloroform and ethyl acetate, and dried in a vacuum. Yield: 20 mg (63%). mp > 300°C. IR (ATR), ν/cm^{-1}: 3021 (Ar–H), 2967–2877 (Aliph. C–H), 1590, 1452, 1387, 1334, 1291, 1255, 1122, 1058, 910, 871, 833, 759, 688. UV–Vis (DMF) λmax (logε): 673 (4.96), 608 (4.25), 356 (4.54). MALDI-TOF-MS (*m/z*) calcl. 4085.23; found: 383.99 $[M\text{-}8I]^{+8}$.

3 | Results and Discussion

3.1 | Synthesis and Characterization

The synthesis of targeted **EA-TD-Si** and **EA-TD-SiQ** is shown in Figure 1. Firstly, **EA-D-OH** [21] was mixed in chloroform in the presence of $SOCl_2$, and thus, the benzylic OH group was chlorinated to obtain the **EA-D-Cl**. **EA-TD-OH** was synthesized by a nucleophilic substitution reaction by mixing **EA-D-Cl** and 3,5-dihydroxybenzylalcohol in acetone at reflux temperature in the presence of potassium carbonate and 18-crown-6. **EA-TD-Si** was prepared from **EA-TD-OH,** $SiPcCl_2$, and NaH as a

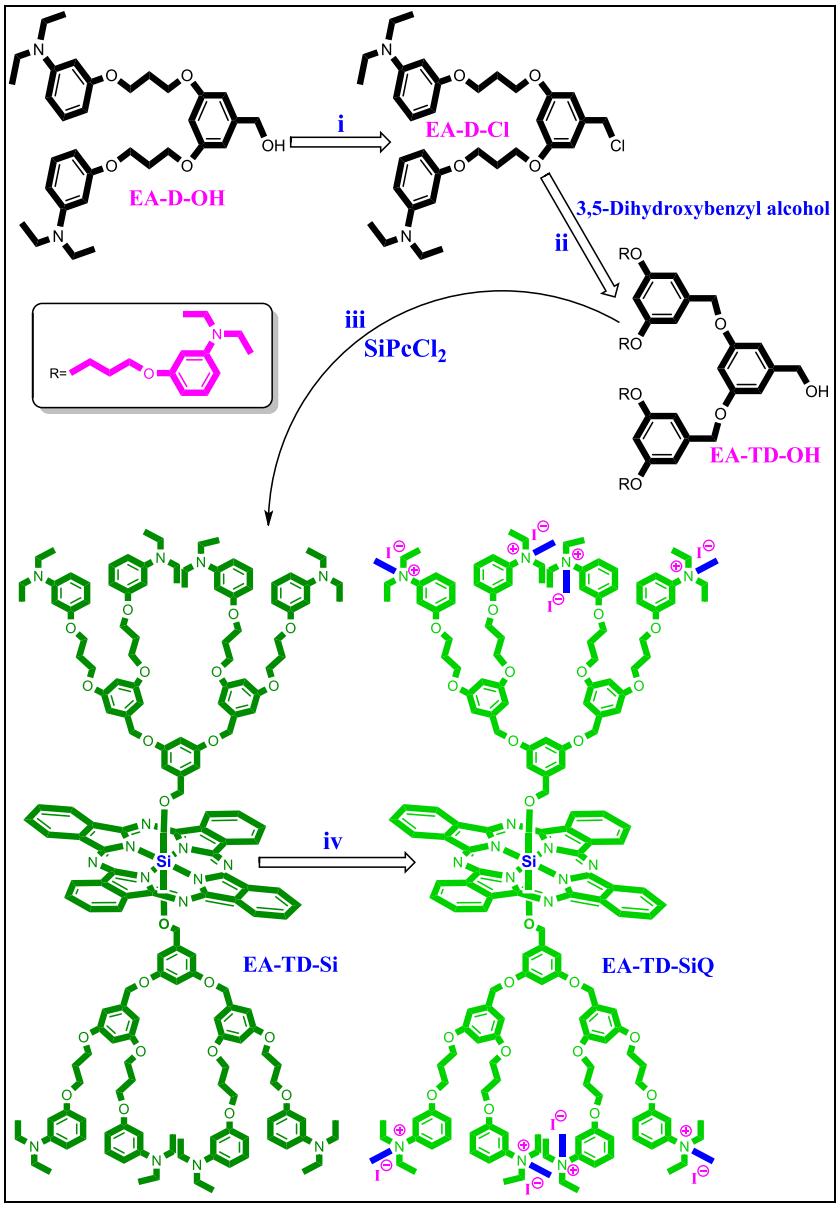

FIGURE 1 | Synthesis pathway of targeted compounds. (i) $SOCl_2$ and $CHCl_3$. (ii) Acetone, 18-crown-6, and K_2CO_3. (iii) NaH and toluene. (iv) CH_3I and chloroform.

base in toluene at 110°C. To synthesize the water-soluble axially disubstituted silicon compounds (**EA-TD-SiQ** and **EA-TD-Si),** CH_3I was mixed in chloroform in the dark for 4 days. The new **EA-D-Cl**, **EA-TD-OH**, **EA-TD-Si**, and **EA-TD-SiQ** were characterized by the necessary spectroscopic methods (^{1}H-NMR, ^{13}C-NMR, FT-IR, MS, MALDI-TOF, and UV–Vis). In the IR spectrum of the **EA-D-Cl**, the benzylic –OH stretching vibration was eliminated as a result of the chlorination reaction. Additionally, aromatic sp^2 and sp^3 carbon vibrations were observed at 3087 and 2963–2850 cm^{-1}, respectively. In the ^{1}H-NMR spectrum of the **EA-D-Cl**, the peak of the –OH proton of the **EA-D-OH** disappeared. Looking at the ^{13}C-NMR spectrum, aromatic carbons and aliphatic carbons of the **EA-D-Cl** appeared in the range of 160.20–98.61 ppm and 67.78–12.87 ppm, respectively. In the mass spectrum, the molecular ion peak at *m/z* 569.36 as M + H supported the proposed structure. In the IR spectrum of **EA-TD-OH**, unlike **EA-D-Cl**, a stretching vibration belonging to the –OH group was seen at 3456 cm^{-1}. In the ^{1}H-NMR spectrum of **EA-TD-OH**, the –OH proton was seen at 5.14 ppm, and its presence was supported by exchange with D_2O. The aromatic and aliphatic protons were seen in the range of 6.98–6.14 ppm and 4.94–1.02 ppm, respectively. Looking at the ^{13}C-NMR spectrum of **EA-TD-OH**, aromatic carbons appeared at 160.18–98.58 ppm, and aliphatic carbons appeared at 69.37–12.81 ppm. In the MS spectrum of **EA-TD-OH**, the molecular ion peak was seen at *m/z* 1205.33 as M^+. When the FT-IR spectrum of the **EA-TD-Si** was examined, aromatic C–H at 3078 cm^{-1}, aliphatic C–H stretching vibration bands at 2965–2871 cm^{-1}, and characteristic Si–O–C vibration at 1060 cm^{-1} were observed. In the ^{1}H-NMR spectrum of **EA-TD-Si** (Figure 2), the characteristic 8

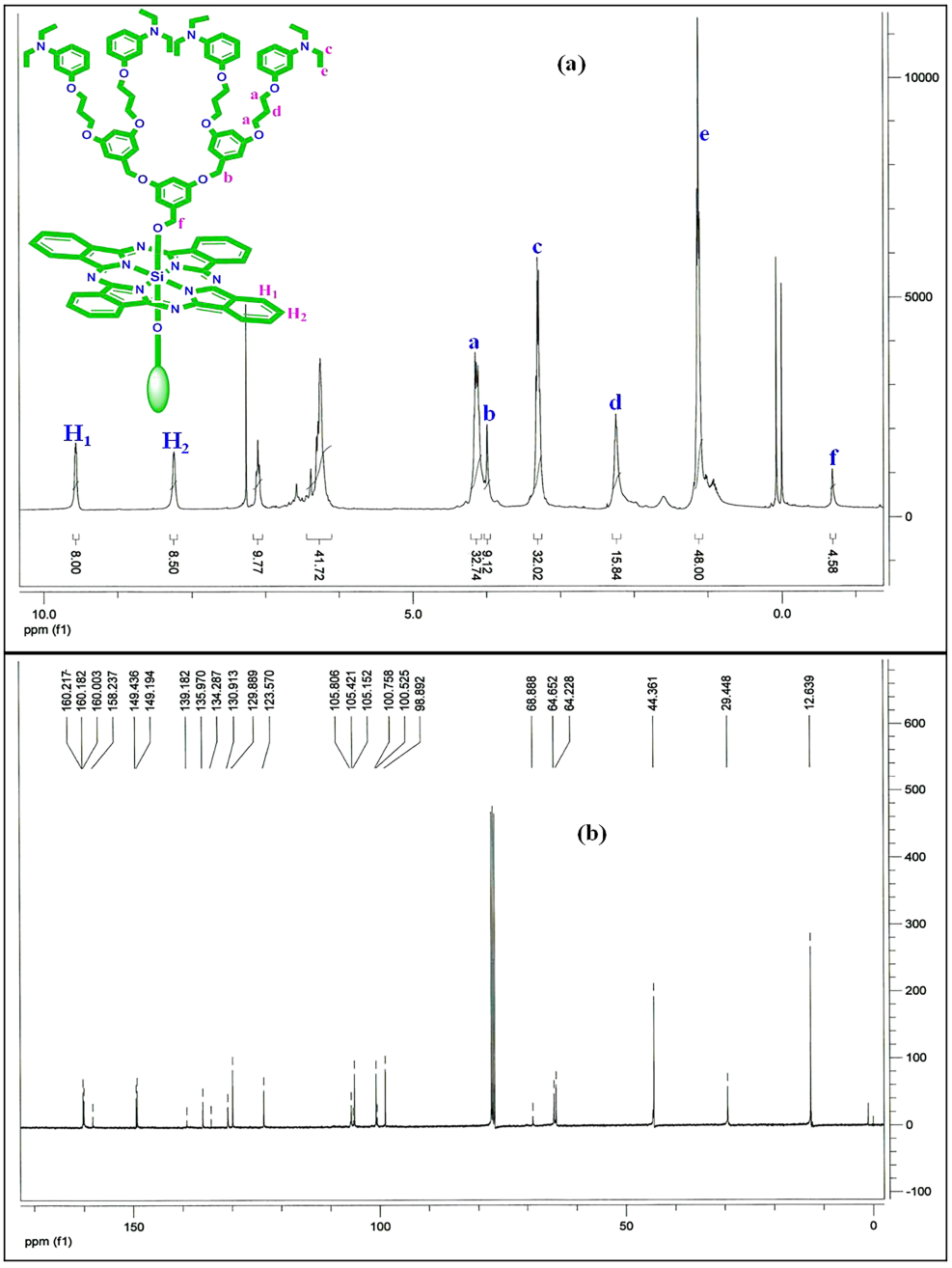

FIGURE 2 | (a) ^{1}H-NMR spectrum of **EA-TD-Si**. (b) ^{13}C-NMR spectrum of **EA-TD-Si**.

alpha and 8 beta protons of the phthalocyanine ring were seen at 9.57 and 8.24 ppm, respectively, as well as aromatic protons at 7.10–6.24 ppm. Protons belonging to the O–CH_2, CH_2–N, –CH_2–, and CH_3 groups appeared at 4.14–3.99, 3.30, 2.24, and 1.12 ppm, respectively. Additionally, it was observed that the protons belonging to the Si–O–CH_2 group were at −0.68 ppm (s, 4H) due to magnetic anisotropy [22]. In the mass spectrum of **EA-TD-Si**, the molecular ion peak was seen at *m/z* 2949.03 $[M]^+$. In the IR spectrum, no differences were shown between **EA-TD-Si** and **EA-TD-SiQ**. Also, the molecular ion peak of **EA-TD-SiQ** was shown at *m/z* = 383.99 $[M\text{-}8I]^{+8}$. The UV–Vis spectra of **EA-TD-Si** and **EA-TD-SiQ** were taken in DMF (Figure 3). The Q bands of **EA-TD-Si** and **EA-TD-SiQ** were shown at 679 and 673 nm. The B bands of **EA-TD-Si** and **EA-TD-SiQ** were displayed at 353 and 356 nm, respectively.

3.2 | DNA Damage/Photodamage of the Compounds

In this study, the supercoiled pBR322 plasmid DNA damage/photodamage effects of **EA-TD-Si** and **EA-TD-SiQ** were examined depending on both concentration and light dose using the agarose gel electrophoresis method. The results are presented in Figure 4. In the work, methylene blue (MB) was used as a positive control. Compounds were dissolved in a final volume of 0.5% DMSO, freshly. Firstly, as shown in Figure 4a, the plasmid DNA damage effects of both compounds were examined due to concentration without light irradiation, and it was revealed that no remarkable DNA damage was observed in the presence of **EA-TD-Si** and **EA-TD-SiQ** against the control group (Figure 4a, Lane 1). Then, photodamage activities on plasmid DNA were examined for 5, 15, 30, and 45 min of light exposure to the presence of **EA-TD-Si** and **EA-TD-SiQ**. In 5 min of light stimulation, no photodamage was observed at the used concentrations of **EA-TD-Si** (1, 10, and 50 μM), while the percentage of Form I decreased and the percentage of Form II increased in the presence of **EA-TD-SiQ** (10 and 50 μM) (Figure 4b). In 15 min of light exposure, plasmid DNA was completely degraded in the presence of **EA-TD-SiQ** at 50 μM (Figure 4c, Lane 7). In the presence of MB used as a positive control at the same concentration, the percentage of Form II of plasmid DNA was calculated at 100% (Figure 4c, Lane 10). When the light treatment time was increased to 30 min, plasmid DNA was completely degraded at 10 μM as well as 50 μM in the presence of **EA-TD-SiQ** (Figure 4d, Lanes 6 and 7). On the other hand, no photodamage was observed in the presence of **EA-TD-Si**. Finally, when the light exposure time was 45 min, plasmid DNA was completely degraded at all concentrations of **EA-TD-SiQ** (Figure 4e, Lanes 5–7), while **EA-TD-Si** did not show any photodamage on plasmid DNA (Figure 4e, Lanes 2–4). The results revealed that **EA-TD-SiQ** caused stronger damage to plasmid DNA compared to MB. This is thought to be due to the higher solubility of **EA-TD-SiQ** in water and its higher reactive oxygen species generation in the buffer.

There are studies in the literature showing that silicon (IV) phthalocyanines containing different substitute groups cause DNA photodamage. In one of these, Gümüşgöz Çelik et al. reported that axially symmetric and unsymmetric silicon (IV)

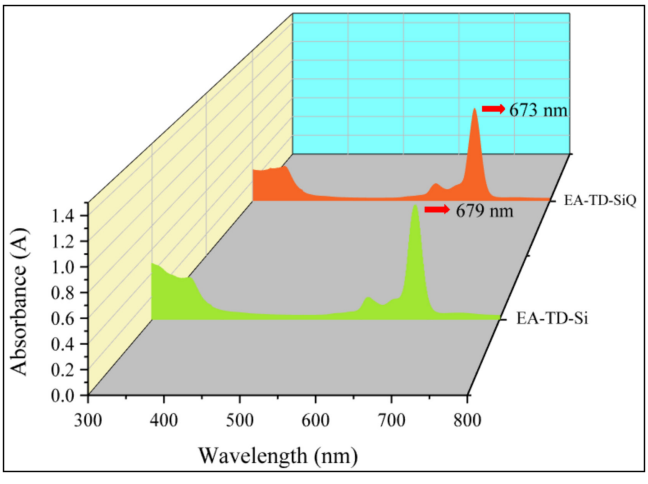

FIGURE 3 | UV–Vis spectra of **EA-TD-Si** and **EA-TD-SiQ** in DMF.

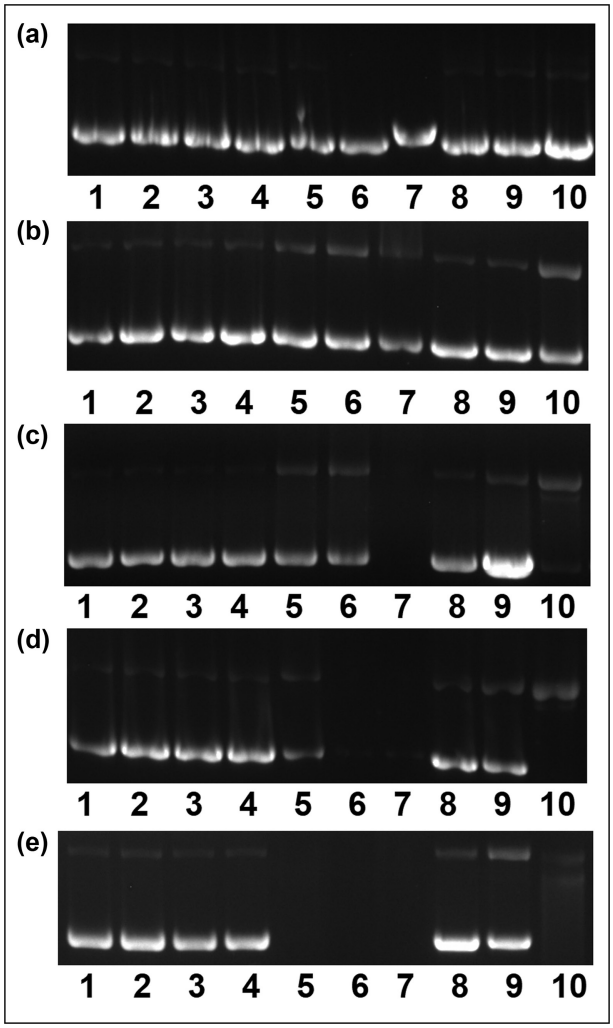

FIGURE 4 | Plasmid DNA damage effects of compounds (a) 30 min at dark, (b) 5 min of light irradiation, (c) 15 min of light irradiation, (d) 30 min of light irradiation, and (e) 45 min of light irradiation (light: white; dose: 17.5 mW/cm^2). Lane 1: DNA control; Lanes 2–4: DNA + **EA-TD-Si** (1, 10, and 50 μM, respectively); Lanes 5–7: DNA + **EA-TD-SiQ** (1, 10, and 50 μM, respectively); Lanes 8–10: DNA + MB (1, 10, and 50 μM, respectively).

phthalocyanines bearing anti-inflammatory groups showed excellent nuclease activity on plasmid DNA [23]. In another study, Farajzadeh et al. reported that quaternized axially disubstituted silicon (IV) phthalocyanines (**1-3SiQ**) cleaved the supercoiled form into nicked form in the dark [24]. In our group's study, 1-acetylpiperazine substituted silicon (IV) phthalocyanine had significant photo nuclease actions on plasmid DNA [25]. All these studies revealed that silicon phthalocyanine bearing different substituted groups can cause damage to plasmid DNA without light exposure.

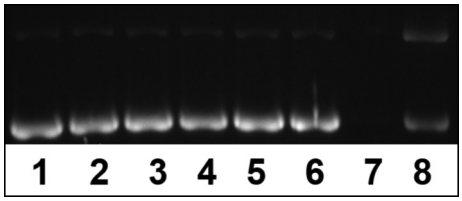

FIGURE 5 | Supercoiled pBR322 plasmid DNA nuclease in the presence of DMSO and NaN_3 in the absence and presence of **EA-TD-SiQ** in the buffer (Tris-HCl pH 7.0). Lane 1: DNA control; Lane 2: DNA control + 30 min light; Lane 3: DNA + DMSO (0.4 mM); Lane 4: DNA + NaN_3 (0.4 mM); Lane 5: DNA + DMSO (0.4 mM) + 30 min light; Lane 6: DNA + NaN_3 (0.4 mM) + 30 min light; Lane 7: DNA + DMSO (0.4 mM) + **EA-TD-SiQ** (10 μM) + 30 min light; Lane 8: DNA + NaN_3 (0.4 mM) + **EA-TD-SiQ** (10 μM) + 30 min light.

3.3 | DNA Photodamage Mechanism in the Presence of the Compounds

In this study, DMSO (hydroxyl radical scavenger) and NaN_3 (singlet oxygen scavenger) were used to determine the reactive oxygen species that cause plasmid DNA photodamage in the presence of **EA-TD-SiQ** with light irradiation. The results are shown in Figure 5. As can be seen in Figure 5, DMSO and NaN_3 did not show any damage to plasmid DNA without light exposure. In Figure 5, Lanes 7 and 8, the band intensity was analyzed after the addition of 10 μM of **EA-TD-SiQ** followed by 30 min of light irradiation. The results indicated that the band intensity completely disappeared (Figure 5, Lane 7), while Form I was observed in Figure 5, Lane 8. This revealed that **EA-TD-SiQ** showed photodamage on DNA by generating singlet oxygen in the presence of light irradiation.

3.4 | Cytotoxic and Phototoxic Properties of the Compounds

In this work, the cytotoxic and phototoxic properties of **EA-TD-Si** and **EA-TD-SiQ** were investigated using an MTT assay on HEC-1B (HTB-113™, ATCC) human endometrium adenocarcinoma. In this study, BEAS-2B (human bronchial epithelial cells) (CRL-9609™, ATCC) was used as a healthy cell line. The results are presented in Figure 6, and MB was used as a positive control. Cells were treated with various concentrations

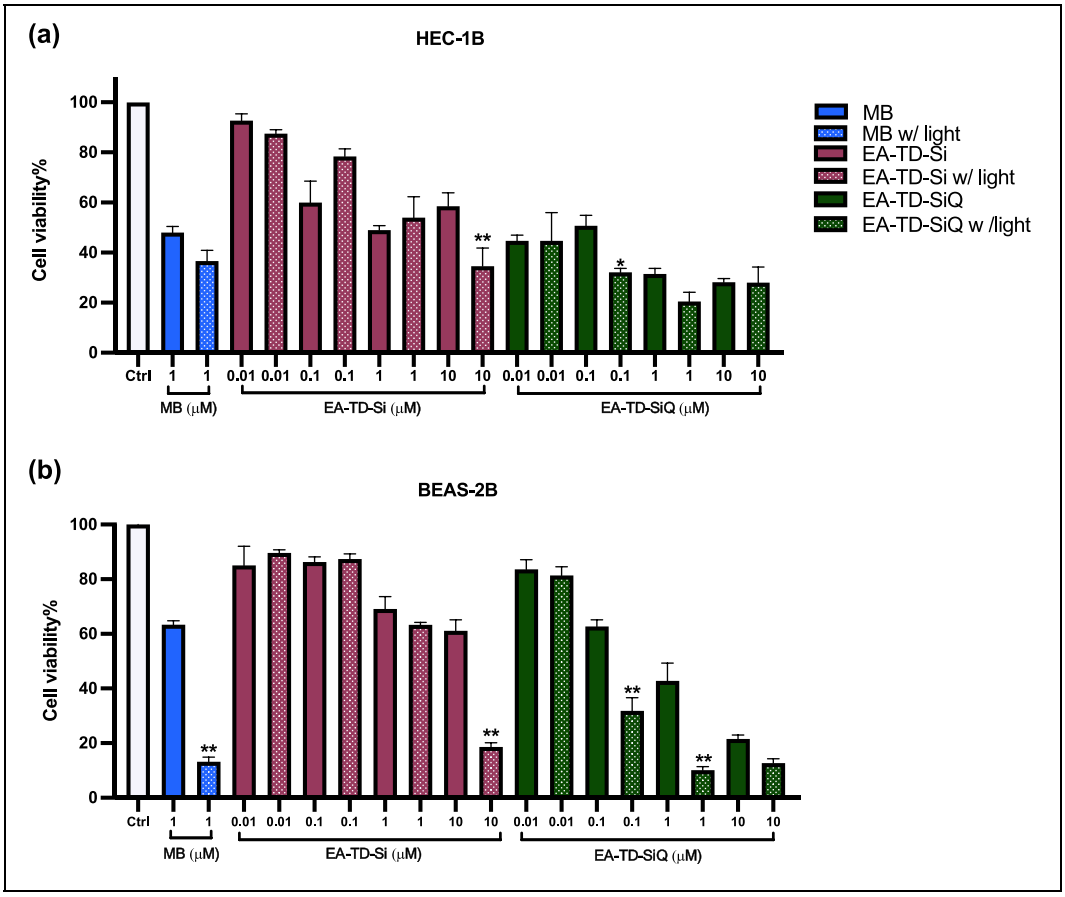

FIGURE 6 | Cytotoxicity/phototoxicity profile of the compounds in HEC-1B (a) and BEAS-2B (b) cells for 24 h. Statistical differences between control vs. groups $^*p < 0.01$; $^{**}p < 0.0001$. Ctrl: control (DMSO 0.5%, v/v); MB: methylene blue. (Light: white; dose: 17.5 mW/cm^2; time: 60 min.).

(0.01–10 μM) of **EA-TD-Si** and **EA-TD-SiQ**, freshly diluted with cell culture medium containing 0.5% (v/v) DMSO. As a positive control, MB (Isolab, Germany) was used at 1 μM in a dissolved DMSO as described previously. According to the MTT assay, exposure to the highest tested concentration of **EA-TD-Si** (10 μM) for 24 h to HEC-1B (Figure 6a) and BEAS-2B cells (Figure 6b) showed significant phototoxicity when the cells were exposed to light irradiation (white, 17.5 mW/cm^2, 60 min) compared to the nonirradiated group. However, 0.1 and 1 μM **EA-TD-SiQ** exposure to BEAS-2B cells showed higher phototoxicity compared to the same concentration exposure in HEC-1B cells. Moreover, the phototoxic action of 10 μM **EA-TD-SiQ** was statistically not significant compared to the nonirradiated group in BEAS-2B cells, though there was a notable decline in the cell viability (Figure 6b). In addition, for **EA-TD-SiQ**, 1 μM exposure in HEC-1B cells exhibited reduced cell viability when light irradiation was applied. These results showed that **EA-TD-SiQ** had higher phototoxic activity on the HEC-1B cell line than both the positive control and **EA-TD-Si** at a concentration of 1 μM. The reason why **EA-TD-SiQ** shows higher efficiency can be thought to be its better solubility, thanks to the ammonium groups in its structure.

While research has revealed that there are no studies on phthalocyanines and EC cells, it has been revealed in the literature that there are many studies on gynecological cancer cells. Hodgkinson et al. reported that the effect of PDT in the presence of sulfonated zinc phthalocyanine Ps ($ZnPcS_{mix}$) was examined by irradiating cervical cancer (HeLa) cells with light (8 J/cm^2, 673 nm). The results showed that the cell viability decreased by 25% with light irradiation in the presence of $ZnPcS_{mix}$ [26]. In another study, Göksel, Durmuş, and Biyiklioglu reported that the water-soluble silicon (IV) phthalocyanine derivatives exhibited cytotoxicity on HeLa cells [27]. Yurttaş et al. reported the cytotoxic effect and molecular basis of L1ZnPc (2,9,16,23-tetrakis(4-carboxyethylsulphanyl)phthalocyaninatozinc (II)) on HeLa cells [28, 29]. The cell viability was about 30% in the presence of L1ZnPc with light exposure (5 mJ/cm^2), and HeLa cells were driven to death through apoptosis. All these studies revealed that phthalocyanines are promising candidates for the treatment of gynecological diseases. In this study, the effects of **EA-TD-SiQ** on HEC-1B cells formed an idea about its usability in the treatment of this disease.

4 | Conclusion

In summary, we synthesized axially bis-{3,5-bis[(3,5-bis{3-[3 (diethylamino)phenoxy]propoxy}benzyl)oxy]phenyl}methoxy group substituted silicon phthalocyanine and its water-soluble derivative. The supercoiled pBR322 plasmid DNA damage effects of **EA-TD-Si** and **EA-TD-SiQ** were examined using agarose gel electrophoresis without irradiation. Then, the reactive oxygen species produced by the **EA-TD-SiQ** in the presence of light were determined. Finally, the cytotoxic and phototoxic activities of **EA-TD-Si** and **EA-TD-SiQ** on HEC-1B cells were examined using the MTT assay. The results determined that **EA-TD-SiQ** showed high photodamage properties depending on the light dose. It has also been determined that **EA-TD-SiQ** damaged DNA by producing singlet oxygen in the presence of light. According to the MTT assay, when **EA-TD-SiQ** (1 μM) is exposed to light, cell viability decreases to approximately 20% in HEC-1B cells. This result was found to be quite high compared to **EA-TD-Si**. In light of all these results, it is thought that the **EA-TD-SiQ** has the potential to be used in EC treatment, and the mechanism can be elucidated with detailed studies.

Author Contributions

Turgut Keles: investigation, methodology. **Gökçe Seyhan:** investigation, methodology. **Zekeriya Biyiklioglu:** writing – original draft, writing – review and editing, supervision. **Kübra Kolci:** investigation, methodology. **Rengin Reis:** writing – original draft, supervision. **Burak Barut:** investigation, writing – original draft, supervision.

Acknowledgments

The authors have nothing to report.

Data Availability Statement

The data that support the findings of this study are available from the corresponding author upon reasonable request.

References

1. World Cancer Research Fund International, Endometrial Cancer Statistics, accessed April 01, 2024, https://www.wcrf.org/cancer-trends/endometrial-cancer-statistics/.

2. C. Bosch Solanes, Photodynamic Therapy as an Alternative to Progestogens in Endometrial Cancer Grade 1A G1: Multicenter Clinical Analysis (2022).

3. Y. Wang, S. Chen, C. Wang, and F. Guo, "Nanocarrier-Based Targeting of Metabolic Pathways for Endometrial Cancer: Status and Future Perspectives," *Biomedicine & Pharmacotherapy* 166 (2023): 115348.

4. A. Saito, H. Yoshida, T. Nishikawa, and K. Yonemori, "Human Epidermal Growth Factor Receptor 2 Targeted Therapy in Endometrial Cancer: Clinical and Pathological Perspectives," *World Journal of Clinical Oncology* 12 (2021): 868–881.

5. S. M. Kim, Y. H. Rhee, and J. S. Kim, "The Anticancer Effects of Radachlorin-Mediated Photodynamic Therapy in the Human Endometrial Adenocarcinoma Cell Line HEC-1-A," *Anticancer Research* 37 (2017): 6251–6258.

6. M. Rubinstein, S. Shen, B. J. Monk, et al., "Looking Beyond Carboplatin and Paclitaxel for the Treatment of Advanced/Recurrent Endometrial Cancer," *Gynecologic Oncology* 167 (2022): 540–546.

7. M. Nowak-Perlak, P. Ziółkowski, and M. Woźniak, "A Promising Natural Anthraquinones Mediated by Photodynamic Therapy for Anti-Cancer Therapy," *Phytomedicine* 119 (2023): 155035.

8. Y. He, L. Luo, and L. Liu, "Photodynamic Therapy for Treatment of Burns: A System Review and Meta-Analysis of Animal Study," *Photodiagnosis and Photodynamic Therapy* 45 (2024): 103905.

9. S. Nath, M. A. Saad, M. Pigula, J. W. Swain, and T. Hasan, "Photoimmunotherapy of Ovarian Cancer: A Unique Niche in the Management of Advanced Disease," *Cancers* 11 (2019): 1887.

10. J. H. Correia, J. A. Rodrigues, S. Pimenta, T. Dong, and Z. Yang, "Photodynamic Therapy Review: Principles, Photosensitizers, Applications, and Future Directions," *Pharmaceutics* 13 (2021): 1332.

11. C. Donohoe, M. O. Senge, L. G. Arnaut, and L. C. Gomes-da-Silva, "Cell Death in Photodynamic Therapy: From Oxidative Stress to Anti-Tumor Immunity," *Biochimica et Biophysica Acta (BBA)-Reviews on Cancer* 1872 (2019): 188308.

12. G. H. Raab, A. F. Schneider, W. Eiermann, H. Gottschalk-Deponte, R. Baumgartner, and W. Beyer, "Response of Human Endometrium and Ovarian Carcinoma Cell-Lines to Photodynamic Therapy," *Archives of Gynecology and Obstetrics* 248 (1990): 13–20.

13. X. Schneider-Yin, A. Kurmanaviciene, M. Roth, et al., "Hypericin and 5-Aminolevulinic Acid-Induced Protoporphyrin IX Induce Enhanced Phototoxicity in Human Endometrial Cancer Cells With Non-Coherent White Light," *Photodiagnosis and Photodynamic Therapy* 6, no. 1 (2009): 12–18.

14. P. Ziółkowski, K. Symonowicz, B. J. Osiecka, and J. Gerber, "Photodynamic Treatment of Epithelial Tissue Derived From Patients With Endometrial Cancer: A Contribution to the Role of Laminin and Epidermal Growth Factor Receptor in Photodynamic Therapy," *Journal of Biomedical Optics* 4 (1999): 272–275.

15. M. C. Choi, S. G. Jung, H. Park, Y. H. Cho, L. Chan, and S. J. Kim, "Fertility Preservation via Photodynamic Therapy in Young Patients With Early-Stage Uterine Endometrial Cancer," *International Journal of Gynecological Cancer* 23 (2013): 698–704.

16. H. Godoy, P. Vaddadi, M. Cooper, P. J. Frederick, K. Odunsi, and S. Lele, "Photodynamic Therapy Effectively Palliates Gynecologic Malignancies," *European Journal of Gynaecological Oncology* 34 (2013): 300–302.

17. K. L. M. Santos, R. M. Barros, D. P. da Silva Lima, et al., "Prospective Application of Phthalocyanines in the Photodynamic Therapy Against Microorganisms and Tumor Cells: A Mini-Review," *Photodiagnosis and Photodynamic Therapy* 32 (2020): 102032.

18. G. Karanlık, C. C. Karanlık, G. Y. Atmaca, and A. Erdoğmuş, "Comparative Evaluation of Singlet Oxygen Generation of New Tetra-Schiff Base Substituted Zinc Phthalocyanine by Photochemical and Sonophotochemical Techniques," *Journal of Molecular Structure* 1299 (2024): 137233.

19. K. Janas, E. Boniewska-Bernacka, G. Dyrda, and R. Słota, "Porphyrin and Phthalocyanine Photosensitizers Designed for Targeted Photodynamic Therapy of Colorectal Cancer," *Bioorganic & Medicinal Chemistry* 30 (2021): 115926.

20. S. Gorduk and O. Avciata, "A3B Type Asymmetric Metallo Phthalocyanines Bearing Carboxylic Acid and Tert-Butyl Groups: Photophysical, Photochemical and Aggregation Properties," *Journal of Photochemistry and Photobiology A: Chemistry* 449 (2024): 115387.

21. T. Keleş, B. Barut, A. Özel, and Z. Bıyıklıoğlu, "Design, Synthesis and Biological Evaluation of Water Soluble and Non-Aggregated Silicon Phthalocyanines, Naphthalocyanines Against A549, SNU-398, SK-MEL128, DU-145, BT-20 and HFC Cell Lines as Potential Anticancer Agents," *Bioorganic Chemistry* 107 (2021): 104637.

22. H. Baş, Z. Bıyıklıoğlu, B. Barut, C. Ö. Yalçın, and A. Özel, "Highly Water Soluble Axial Disubstituted Silicon(IV) Phthalocyanine, Naphthalocyanine: Synthesis, DNA Interaction and Anticancer Effects Against Human Lung (A549), Liver (SNU-398), Melanoma (SK-MEL128), Prostate (DU-145), Breast (BT-20) Cell Lines," *Inorganic Chemistry Communications* 156 (2023): 111139.

23. G. Gümüşgöz Çelik, S. Gonca, B. Şahin, S. Özdemir, D. Atilla, and A. G. Gürek, "Novel Axially Symmetric and Unsymmetric Silicon(IV) Phthalocyanines Having Anti-Inflammatory Groups: Synthesis, Characterization and Their Biological Properties," *Dalton Transactions* 51 (2022): 7517–7529.

24. N. Farajzadeh, N. Güler Kuşçulu, H. Y. Yenilmez, D. Bahar, and Z. Altuntaş Bayır, "Anticancer and Biological Properties of New Axially Disubstituted Silicon Phthalocyanines," *Dalton Transactions* 51 (2022): 7539–7550.

25. H. Baş, B. Barut, Z. Biyiklioglu, and A. Özel, "Synthesis, DNA Interaction, Topoisomerase I, II Inhibitory and Cytotoxic Effects of Water Soluble Silicon (IV) Phthalocyanine and Napthalocyanines Bearing 1-Acetylpiperazine Units," *Dyes and Pigments* 160 (2019): 136–144.

26. N. Hodgkinson, C. A. Kruger, M. Mokwena, and H. Abrahamse, "Cervical Cancer Cells (HeLa) Response to Photodynamic Therapy Using a Zinc Phthalocyanine Photosensitizer," *Journal of Photochemistry and Photobiology B: Biology* 177 (2017): 32–38.

27. M. Göksel, M. Durmuş, and Z. Biyiklioglu, "Synthesis and Photodynamic Activities of Novel Silicon(Iv) Phthalocyanines Axially Substituted With Water Soluble Groups Against HeLa Cancer Cell Line," *Dalton Transactions* 50 (2021): 2570–2584.

28. A. G. Yurttaş, A. M. Sevim, K. Çınar, G. Y. Atmaca, A. Erdoğmuş, and A. Gül, "The Effects of Zinc(II)Phthalocyanine Photosensitizers on Biological Activities of Epitheloid Cervix Carcinoma Cells and Precise Determination of Absorbed Fluence at a Specific Wavelength," *Dyes and Pigments* 198 (2022): 110012.

29. A. G. O. K. Yurttas, Z. Okat, T. Elgun, K. U. C. A. R. Cifci, A. M. Sevim, and A. Gul, "Genetic Deviation Associated With Photodynamic Therapy in HeLa Cell," *Photodiagnosis and Photodynamic Therapy* 42 (2023): 103346.

Supporting Information

Additional supporting information can be found online in the Supporting Information section.